Geochimica et Cosmochimica Acta, Vol. 69, No. 15, pp. 3747–3758, 2005

0016-7037/05 $30.00 + .00

doi:10.1016/j.gca.2005.03.019

# Diel behavior of rare earth elements in a mountain stream with acidic to neutral pH

CHRISTOPHER H. GAMMONS[1,*], SCOTT A. WOOD[2], and DAVID A. NIMICK[3]

[1]Department of Geological Engineering, Montana Tech of The University of Montana, Butte, Montana 59701, USA
[2]Department of Geological Sciences, University of Idaho, Moscow, Idaho, USA
[3]U. S. Geological Survey, Helena, Montana, USA

(*Received November 24, 2004; accepted in revised form March 1, 2005*)

**Abstract**—Diel (24-h) changes in concentrations of rare earth elements (REE) were investigated in Fisher Creek, a mountain stream in Montana that receives acid mine drainage in its headwaters. Three simultaneous 24-h samplings were conducted at an upstream station (pH = 3.3), an intermediate station (pH = 5.5), and a downstream station (pH = 6.8). The REE were found to behave conservatively at the two upstream stations. At the downstream station, REE partitioned into suspended particles to a degree that varied with the time of day, and concentrations of dissolved REE were 2.9- to 9.4-fold (190% to 830%) higher in the early morning vs. the late afternoon. The decrease in dissolved REE concentrations during the day coincided with a corresponding increase in the concentration of REE in suspended particles, such that diel changes in the total REE concentrations were relatively minor (27% to 55% increase at night). Across the lanthanide series, the heavy REE partitioned into the suspended solid phase to a greater extent than the light REE. Filtered samples from the downstream station showed a decrease in shale-normalized REE concentration across the lanthanide series, with positive anomalies at La and Gd, and a negative Eu anomaly. As the temperature of the creek increased in the afternoon, the slope of the REE profile steepened and the magnitude of the anomalies increased.

The above observations are explained by cyclic adsorption of REE onto suspended particles of hydrous ferric and aluminum oxides (HFO, HAO). Conditional partition coefficients for each REE between the suspended solids and the aqueous phase reached a maximum at 1700 hours and a minimum at 0700 hours. This pattern is attributed to diel variations in stream temperature, possibly reinforced by kinetic factors (i.e., slower rates of reaction at night than during the day). Estimates of the enthalpy of adsorption of each REE onto suspended particles based on the field results averaged +82 kJ/mol and are similar in magnitude to estimates in the literature for adsorption of divalent metal cations onto clays and hydrous metal oxides. The results of this study have important implications to the use of REE as hydrogeochemical tracers in streams. 

## 1. INTRODUCTION

The geochemistry of rare earth elements (REE) in acidic waters has recently received considerable attention (Miekeley et al., 1992; Johannesson and Lyons, 1995; Lewis et al., 1997; Leybourne et al., 1998, 2000; Elbaz-Poulichet and Dupuy, 1999; Hollings et al., 1999; Verplanck et al., 1999, 2004; Johannesson and Zhou, 1999; Gimeno et al., 2000; Åström, 2001; Worrall and Pearson, 2001a, b; Gammons et al., 2003; Wood et al., 2005). The mobilities of REE typically are much higher in acidic as opposed to neutral or alkaline water, making analytical quantification relatively straightforward. REE may be useful as hydrogeochemical tracers of processes occurring near the source of acid generation or in downgradient waters where the acidity is neutralized or diluted. In certain applications—for example, in watersheds draining abandoned mine lands—the potential exists to use REE concentration patterns as fingerprints to discriminate between multiple sources of contamination. However, deposition of hydrous oxides of Fe, Al, and Mn in downstream reaches of mining-impacted waters can lead to sequestration of REE, with attendant interelement fractionation (Verplanck et al., 2004).

Meanwhile, recent work—unrelated to REE—has documented the phenomenon of diel (24-h) cycling of metals in streams of the Northern Rocky Mountains, especially those streams that have been affected by hard-rock mining. In streams with acidic pH, diel metal cycling is dominated by light-sensitive Fe redox reactions (McKnight et al., 1988; McKnight and Bencala, 1989; Sullivan et al., 1998; McKnight et al., 2001; Gammons et al., 2005). In streams with near-neutral to alkaline pH, the concentrations of dissolved metal cations (e.g., $Zn^{2+}$, $Mn^{2+}$, $Cd^{2+}$) tend to increase at night and decrease during the day (Brick and Moore, 1996; Nimick et al., 2003; Jones et al., 2004; Gammons et al., 2005; Nimick et al., 2005). In contrast, anionic constituents (such as $HAsO_4^{2-}$) typically show the reverse trend (Fuller and Davis, 1989; Brick and Moore, 1996; Nimick et al., 1998, 2003). These diel variations are thought to be caused by reversible pH- and temperature-dependent adsorption of ions onto benthic or suspended solid substrates, including biofilms and secondary hydrous metal oxide precipitates (Fuller and Davis, 1989; Nimick et al., 2003; Jones et al., 2004). In many cases, the 24-h fluctuations are quite large and therefore can have important implications as to how the water quality of streams draining abandoned mines should be monitored and assessed.

Given the ongoing interest in the geochemistry of REE in streams and the increased recognition of the importance of diel metal cycling, it is logical to explore the diel behavior of REE in streams. In a companion paper, Gammons et al. (2005)

* Author to whom correspondence should be addressed (cgammons@mtech.edu).

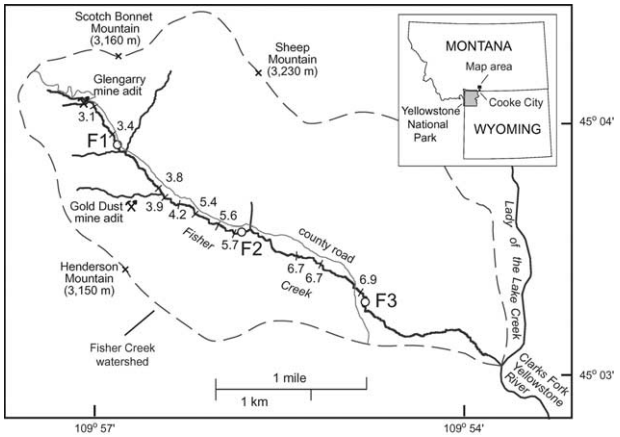


Fig. 1. Diel monitoring stations (*open circles*) and reconnaissance pH values (*short lines*) measured on August 12, 2002, Fisher Creek, New World mining district, Montana.

documented large (as much as sevenfold) diel changes in the dissolved concentration of Fe, Cu, Al, Zn, and Mn in Fisher Creek, a mountain stream whose pH changes from highly acidic to near-neutral over a relatively short distance. The present paper builds on our previous study by determining diel variations in dissolved and total concentrations of REE in Fisher Creek. Possible reasons for the observed trends are evaluated and discussed.

## 2. DESCRIPTION OF THE FIELD AREA AND PREVIOUS WORK

Fisher Creek is a small, high-altitude mountain stream located in the New World mining district, just north of Cooke City, Montana (Fig. 1). The headwaters of Fisher Creek are acidic owing to natural acid rock drainage (Kimball et al., 1999) as well as drainage associated with abandoned mines that produced Cu-Au-Ag-Pb-Zn ore (Elliot et al., 1992). The stream drains an approximately 8-km$^2$ area between 2500 and 3230 m in elevation. Downstream from the Glengarry adit, the pH of Fisher Creek increases owing to the inflow of tributaries and groundwater with near-neutral pH (see Fig. 1). Ocherous secondary precipitates are present over the entire length of Fisher Creek. These precipitates are bright orange-red in the upper acidic reaches and a duller brownish color downstream where pH is higher. This change in color reflects a switch in mineralogy from predominantly hydrous ferric oxide (HFO) in the headwaters to a mixture of HFO and hydrous aluminum precipitates further downstream (Gammons et al., 2005).

General aspects of the hydrogeochemistry of Fisher Creek have previously been described (Amacher et al., 1993, 1995; Amacher, 1998; Kimball et al., 1999; Gammons et al., 2005). Of most relevance to the present paper is the study of Gammons et al. (2005), who conducted three simultaneous 24-h samplings in August 2002 at an upstream, intermediate, and downstream location (F1, F2, and F3, respectively) on Fisher Creek (Fig. 1). The 24-h average pH varied from 3.3 (F1) to 5.5 (F2) to 6.8 (F3). Thus, diel metal cycling was investigated simultaneously in three different pH regimes within the same stream system. Despite the steep downstream gradient in pH, the 24-h change in pH at each station was remarkably small ($\pm$0.1 pH units or less). The present study is based on additional analysis of the samples described by Gammons et al. (2005).

## 3. METHODS

### 3.1. Field Methods

All samples analyzed in this study were collected during the diel investigation of Fisher Creek conducted August 13–14, 2002. Gammons et al. (2005) describe the collection of samples and field measurements; only a brief summary is included here.

Water temperature, pH, specific conductance (SC), dissolved oxygen, and streamflow were measured hourly at the three stations on Fisher Creek. Filtered and unfiltered water samples were collected hourly using automated samplers and were processed on site within 5 min of sampling. Filtered samples were processed using disposable 0.1-$\mu$m cellulose-ester membranes. In addition, several samples from each station were filtered through a tangential-flow ultrafilter with a nominal pore size of 10,000 Da ($\sim$0.001 $\mu$m) to test for the presence of colloidal solids. All samples for metal and REE analysis were collected in acid-washed 250-mL high-density polyethylene bottles and were acidified in the field to 0.4% v/v with ultrapure $HNO_3$. Quality-assurance protocols included collection of field duplicates and filtered and unfiltered blanks.

### 3.2. Analytical Methods

All samples were analyzed for a suite of major and trace metals, alkalinity, anions, and $Fe^{2+}/Fe^{3+}$ speciation at the U. S. Geological Survey laboratory, Boulder, Colorado. Methods and analytical data are given in Gammons et al. (2005). Selected samples were later analyzed for a full suite of REE by ICP-MS at Washington State University, Pullman, Wash. Samples analyzed from F3 included all of the filtered and ultrafiltered samples, and every other raw (unfiltered) sample. A smaller number of samples from F1 and F2 also were analyzed for a full suite of REE.

The concentrations of all REE except Pm were determined at Washington State University using a *ThermoFinnigan Element 2* ICP-MS. Neither preconcentration nor dilution was required for analysis. Indium and rhenium were used as internal standards. The following masses were monitored: $^{139}$La, $^{140}$Ce, $^{141}$Pr, $^{146}$Nd, $^{147}$Sm, $^{151}$Eu, $^{157}$Gd, $^{159}$Tb, $^{163}$Dy, $^{165}$Ho, $^{166}$Er, $^{169}$Tm, $^{174}$Yb, and $^{175}$Lu. The masses were selected and the forward power and argon flow rates for the plasma were adjusted to minimize isobaric oxide interferences. However, corrections were necessary for $^{151}$Eu owing to $^{135}$Ba$^{16}$O interference in all samples, and for $^{157}$Gd owing to interference from $^{141}$Pr$^{16}$O in many of the samples. The ICP-MS was calibrated using standards containing 0.08, 0.4, 2, and 8 $\mu$g/L of each REE. Quality control was maintained by analyzing two midlevel standards and a blank every ten samples in the analysis. Data were reprocessed offline using a standardized spreadsheet. Instrument detection limits (IDL) were determined by analyzing 10 instrument blanks (acidified 18 M$\Omega$-cm deionized water). The standard deviation of instrument-blank concentrations for each analyte was multiplied by the Student's *t* at the 99% confidence level (2.821) to calculate the IDL, which ranged from $\sim$0.2 to 1.9 ng L$^{-1}$ depending on the REE.

Analysis of the field duplicate sample (analyzed out of sequence) agreed within $\pm$30% for all REE with the exception of Tm (63%) and Lu (33%); for the elements La through Sm, the agreement was within $\pm$2%. The raw (unfiltered) field blank had total lanthanide concentrations that were $<$6% of the lowest REE concentration in the unfiltered environmental samples. The filtered field blank had dissolved lanthanide concentrations that were $<$25% of the lowest dissolved REE concentration for all REE except Eu, Tm, and Lu. Overall, the quality-control results for Tm and Lu were problematic, owing in part to the very low concentrations of these elements.

## 4. RESULTS

Results for Fe, Cu, Al, Mn, Zn during the 2002 study of Fisher Creek have been previously described, as were diel

Table 1. Average concentrations ($\mu$g/L) of REE in Fisher Creek at F1, F2, and F3. n = number of samples analyzed; RA = raw-acidified; FA = filtered (0.1 $\mu$m)-acidified; UFA = ultrafiltered (0.001 $\mu$m)-acidified; IDL = instrument detection limit.

| Sample type | n | La | Ce | Pr | Nd | Sm | Eu | Gd |
|---|---|---|---|---|---|---|---|---|
| F1-RA | 3 | 4.86 | 10.1 | 1.20 | 4.79 | 0.864 | 0.217 | 1.05 |
| F1-FA | 3 | 4.74 | 9.81 | 1.17 | 4.67 | 0.844 | 0.210 | 1.01 |
| F2-RA | 3 | 1.53 | 2.85 | 0.361 | 1.42 | 0.256 | 0.063 | 0.287 |
| F2-FA | 3 | 1.50 | 2.77 | 0.350 | 1.35 | 0.241 | 0.059 | 0.270 |
| F3-RA | 11 | 0.675 | 1.14 | 0.150 | 0.574 | 0.104 | 0.0228 | 0.118 |
| F3-FA | 21 | 0.429 | 0.525 | 0.0597 | 0.213 | 0.0289 | 0.0055 | 0.0337 |
| F3-UFA | 3 | 0.355 | 0.402 | 0.0448 | 0.161 | 0.0208 | 0.0035 | 0.0250 |
| *FA-blank* | *1* | *0.0067* | *0.0084* | *0.0035* | *0.0058* | *0.0009* | *<IDL* | *0.0030* |
| *RA-blank* | *1* | *0.0013* | *0.0017* | *<IDL* | *0.0015* | *0.0004* | *<IDL* | *0.0012* |
| *IDL* | | *0.0007* | *0.0012* | *0.0005* | *0.0004* | *0.0003* | *0.0019* | *0.0007* |

| Sample type | | Tb | Dy | Ho | Er | Tm | Yb | Lu |
|---|---|---|---|---|---|---|---|---|
| F1-RA | 3 | 0.154 | 0.878 | 0.169 | 0.467 | 0.0584 | 0.351 | 0.0468 |
| F1-FA | 3 | 0.148 | 0.854 | 0.164 | 0.452 | 0.0567 | 0.340 | 0.0455 |
| F2-RA | 3 | 0.0411 | 0.243 | 0.0468 | 0.125 | 0.0162 | 0.0964 | 0.0129 |
| F2-FA | 3 | 0.0388 | 0.227 | 0.0439 | 0.117 | 0.0153 | 0.0886 | 0.0121 |
| F3-RA | 11 | 0.0184 | 0.0978 | 0.0191 | 0.0506 | 0.0068 | 0.0397 | 0.0054 |
| F3-FA | 21 | 0.0049 | 0.0206 | 0.0044 | 0.0117 | 0.0014 | 0.0086 | *<IDL* |
| F3-UFA | 3 | 0.0036 | 0.0148 | 0.0032 | 0.0083 | 0.0018 | 0.0060 | *<IDL* |
| *FA-blank* | *1* | *0.0004* | *0.0010* | *0.0003* | *0.0006* | *<IDL* | *0.0008* | *<IDL* |
| *RA-blank* | *1* | *<IDL* | *<IDL* | *<IDL* | *<IDL* | *<IDL* | *<IDL* | *<IDL* |
| *IDL* | | *0.0003* | *0.0004* | *0.0002* | *0.0003* | *0.0004* | *0.0005* | *0.0019* |

variations in field parameters (Gammons et al., 2005). Results of all REE analyses are summarized in the Appendix. Time-averaged concentrations obtained at each station are summarized in Table 1. The samples are designated RA, FA, or UFA, which corresponds to raw-acidified, filtered (0.1$\mu$m)-acidified, and ultrafiltered (0.001 $\mu$m)-acidified. In this paper, the term dissolved is defined as that portion of the total element concentration that was measured in the 0.1-$\mu$m filtrate. Although the ultrafiltered samples give a more accurate indication of the quantities of REE that were truly dissolved, only three UFA samples were collected. A comparison of the FA and UFA concentrations in these samples showed that a significant percentage of the dissolved REE was actually present as fine colloids with diameter between 0.001 and 0.1 $\mu$m (see Table 1). At 1400 hours, the average ratio of (FA − UFA)/FA concentrations for all 12 REE analyzed was 38%. This ratio decreased to 13% at 2100 hours and 6% at 0400 hours.

### 4.1. Downstream Changes in REE Concentrations and Loads

The average concentration of each REE decreased with distance downstream (Table 1). This decrease was largely the result of dilution; the 24-h average streamflows at the F1, F2, and F3 stations were 0.0153, 0.0530, and 0.0749 $m^3/s$, respectively (Gammons et al., 2005). The 4.9-fold increase in flow between F1 and F3 was caused by inflow of groundwater and tributary streams. At each station, flow decreased ~12%–14% during the day, presumably owing to a reduction in influent groundwater by evapotranspiration in the lush riparian wetland bordering the stream. Besides simply diluting the concentrations of metals from upstream sources, the influx of near-neutral groundwater and surface water also raised the pH of Fisher Creek with distance downstream (Fig. 1).

For each station, average total and dissolved loads for each lanthanide element were calculated from the 24-h average concentration and streamflow. The results (Fig. 2) illustrate that changes in loads between F1 and F2 were not discernable and that, therefore, all REE behaved conservatively in this stream reach. This implies that chemical attenuation of REE was negligible in this upstream reach and furthermore that influent surface water and groundwater must have had negligible concentrations of REE. At F1 and F2, the differences between total and dissolved REE concentrations were not significant (all analyses agreed within ±5%). For this reason, only the total REE loads are plotted in Figure 2 for F1 and F2. In contrast to

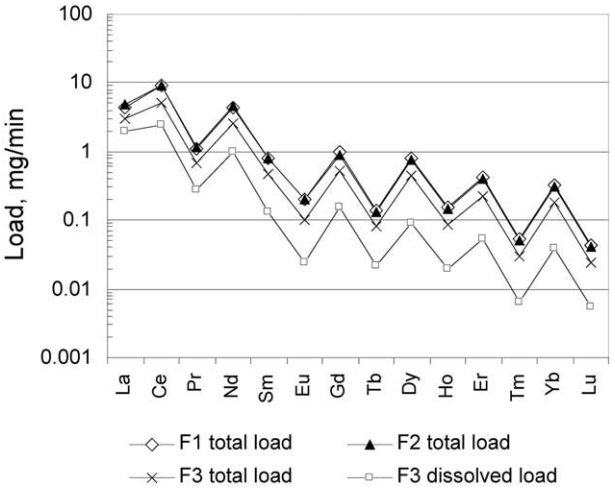


Fig. 2. Calculated loads for each lanthanide element at the upstream (F1), middle (F2), and downstream (F3) stations. The loads represent the average of all samples analyzed for each site. For F1 and F2, the dissolved loads are indistinguishable from the total loads and are omitted for clarity.

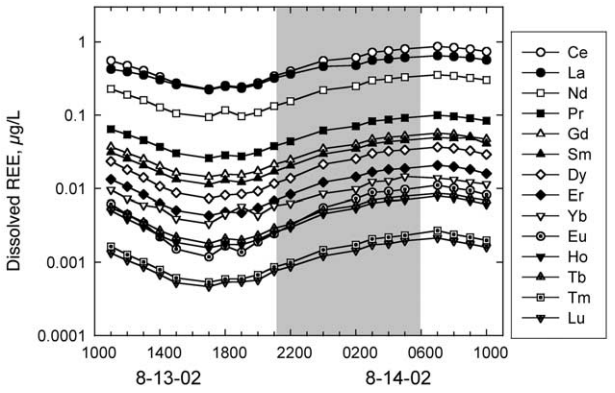


Fig. 3. Diel variation in dissolved REE concentrations at F3. The shaded area denotes nighttime hours.

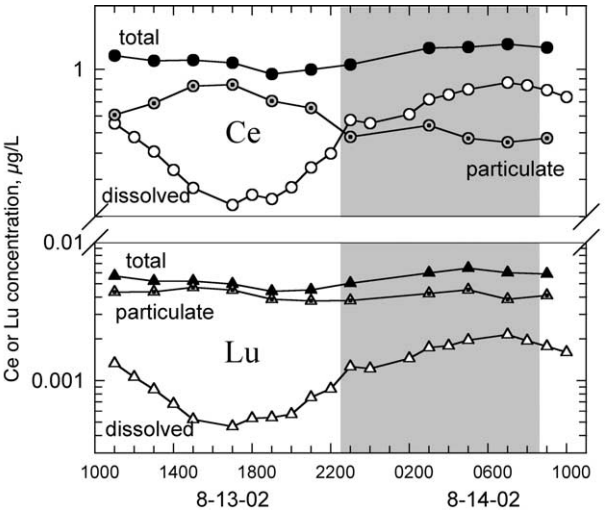


Fig. 4. Diel variations in total, dissolved, and particulate Ce and Lu concentrations at F3. The shaded area denotes nighttime hours.

the upper reach, total loads of all REE decreased consistently (37% to 48%) between F2 and F3. The reduction in dissolved load (59% to 92%) in this reach was even larger. These load decreases indicate that the REE behaved nonconservatively between F2 and F3, most likely by adsorption or mineral precipitation processes.

### 4.2. Diel Changes in REE Concentrations

Whereas diel changes in REE concentrations at F1 and F2 were negligible, all REE exhibited strong diel cycles in dissolved concentration at F3 (Fig. 3). Minimum concentrations occurred in the late afternoon (1700 hours) and maximum concentrations just after sunrise (0700 hours). The average increase in dissolved concentration for all of the REE was 380% (4.8-fold); La had the smallest percentage increase (190%), whereas Eu had the largest increase (840%). The reasons for the anomalous behavior of Eu are not known. Europium anomalies in geologic media may arise from the possibility of reduction of $Eu^{3+}$ to $Eu^{2+}$ (Sverjensky, 1984). It is unlikely that $Eu^{2+}$ could have been stable in Fisher Creek, given the low temperature and oxidized environment (dissolved oxygen concentrations of the water column were close to saturation values at all times). Nonetheless, $Eu^{2+}$ could have been produced as a metastable species by photochemical redox reactions similar to photoreduction of $Fe^{3+}$ to $Fe^{2+}$. We are not aware of a previous study that has documented $Eu^{3+}$ photoreduction in streams and realize that this idea is speculative. It also is possible that the anomalous behavior of Eu was an artifact of analytical difficulties, for example, due to isobaric interferences between Eu and BaO on the ICP-MS. However, the fact that concentrations of dissolved Ba at F3 were rather low (35 to 37 $\mu$g/L) and showed no evidence of diel fluctuation weakens the suggestion that the anomalously large diel concentration changes for Eu were due to BaO isobaric interferences.

Total REE concentrations at F3 showed smaller percentage diel fluctuations than did dissolved REE concentrations. Percentage increases in total REE concentrations during the night varied from 27% (Sm) to 55% (Yb), with an average increase of 37% for all of the lanthanide elements. This implies that most of the REE lost from aqueous solution partitioned into solid particles that remained suspended in the water column. Total, dissolved, and particulate concentrations for Ce and Lu are shown in Figure 4 as examples of the diel concentration trends displayed for all of the REE. The degree to which the REE partitioned into suspended solids varied from element to element and with the time of day (Fig. 5). In general, suspended solids contained the largest fraction of the total REE concentration in the late afternoon (~1700 hours) and the smallest just before dawn (~0500 hours). Figure 5 also shows that, in general, the light REE partitioned to a lesser degree into the solids than did the heavy REE. Again, Eu showed anomalous behavior, with a greater diel fluctuation compared to the other lanthanides.

### 4.3. Shale-Normalized REE Concentration Profiles

To better examine trends across the lanthanide series, the total and dissolved REE concentrations from Fisher Creek were

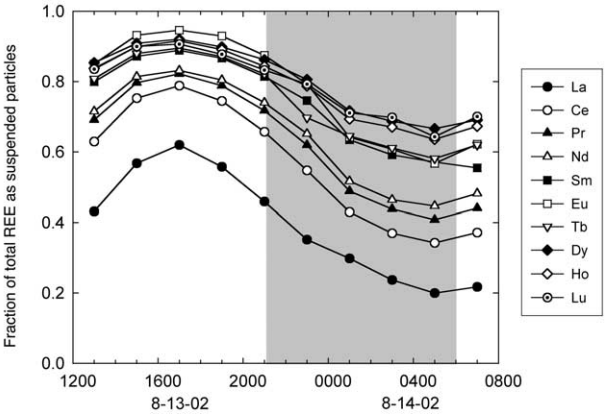


Fig. 5. Diel variation in the fraction of total REE present in water as suspended particles at F3. The elements Er, Tm, and Yb had nearly identical patterns as Lu and have been omitted for clarity. The shaded area denotes nighttime hours.

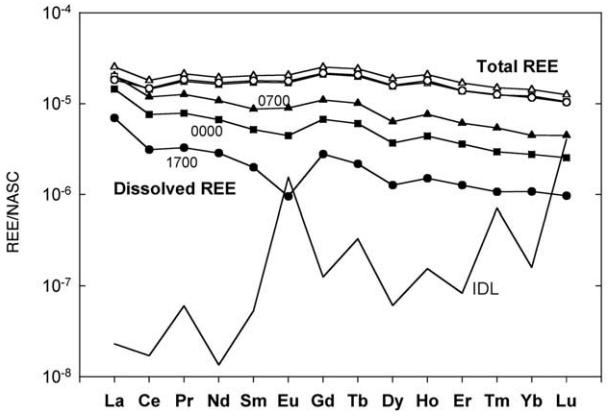


Fig. 6. NASC-normalized REE patterns at F3 for total (open symbols) and dissolved (solid symbols) REE concentrations. Data are shown for 0700, 1700, and 0000 h. IDL indicates the NASC-normalized instrument detection limit.

normalized to the North American Shale Composite, or NASC (Gromet et al., 1984). The profiles for normalized total REE concentrations from F3 (Fig. 6) were generally flat from La to Ho, with slightly lower concentrations for the heavier elements, Er to Lu. Weak negative anomalies were noted at Ce and Dy. The anomalous behavior of Ce may be attributed to its ability to be oxidized to the tetravalent state in oxidized water; however, the Dy anomaly is more difficult to explain. Differences in normalized concentrations with time of day were negligible for the total REE profiles. In the dissolved REE profiles, the Ce and Dy anomalies persist, and a trend is seen of decreasing REE concentration across the series. The slope of the normalized profile was steeper for samples collected in the late afternoon when the REE were partitioning into suspended particles to a greater extent. The dissolved REE profiles also showed a pronounced negative Eu anomaly, which deepened for the samples with the lowest dissolved REE concentration (1700 hours). As discussed above, it is not known whether the Eu anomaly is real or an artifact of analytical difficulties.

### 4.4. Partition Coefficients of REE Between Dissolved and Particulate Phases

The tendency of the REE to partition into suspended solids at F3 was greater in the late afternoon than in the early morning, with the heavy REE having a higher affinity for the solid phase as compared to the light REE (Figs. 6 and 7). Because samples of suspended solids were not collected, it was not possible to directly calculate the distribution coefficients for REE between the dissolved and particulate phases. However, conditional distribution coefficients ($K_d$*) were calculated as follows. First, it was assumed that all partitioning of REE into the solid phase occurred via adsorption onto suspended particles of Fe and Al. (Adsorption onto hydrous Mn oxide was not considered, because suspended Mn particles were negligible at F3.) Next, the concentrations of suspended Fe and Al in each sample were calculated by subtracting the dissolved concentrations from their respective total concentrations. Finally, the Fe and Al particles were assumed to have the approximate stoichiometry of the simple metal hydroxides, $Fe(OH)_3$ and $Al(OH)_3$. Using

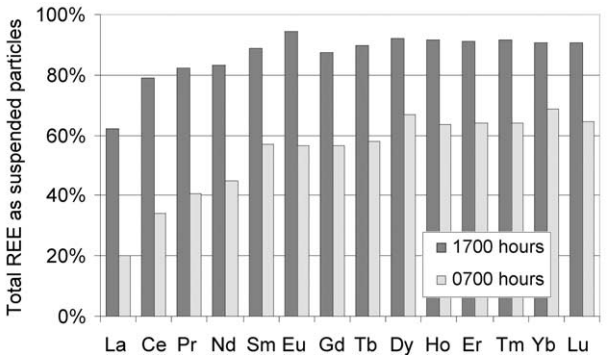


Fig. 7. Variation across the lanthanide series of the percentage of the total REE concentration present as suspended particles at F3. Data are shown for 0700 and 1700 hours for comparison.

these assumptions, values of $K_d$* were calculated for each F3 sample, where:

$$K_d^* = \frac{\mu g/kg \text{ Ln sorbed onto suspended } Me(OH)_3}{\mu g \text{ /L Ln dissolved in water}} \quad (1)$$

Ln refers to any REE and Me refers to either Fe or Al. The derived values of $K_d$* (Fig. 8) varied as a function of time, with greater solid partitioning occurring in the late afternoon compared to the early morning hours. Although these trends are similar to previous diagrams, the $K_d$* values account for changes in the concentration of suspended particles with time at F3. As shown by Gammons et al. (2005), suspended Fe particles were more abundant at F3 during the day, owing to reoxidation of $Fe^{2+}$ produced by photoreduction in upstream reaches. Concentrations of suspended Al particles also showed diel variations, although the maxima and minima occurred roughly 4 hours earlier in the day than for HFO (Gammons et al., 2005).

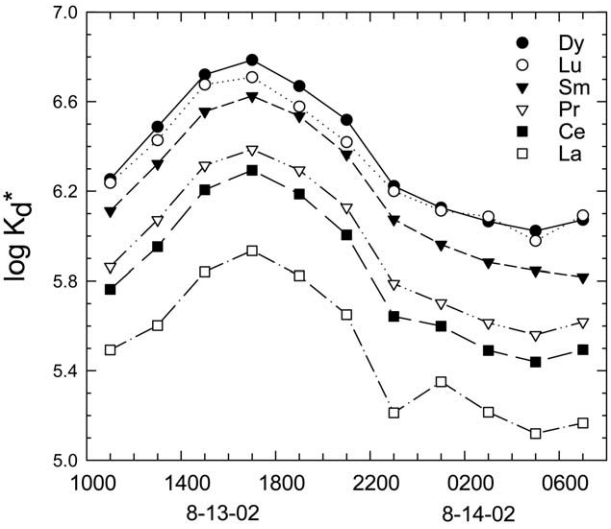


Fig. 8. Diel variation in the value of the conditional distribution coefficient (log $K_d$*) for partitioning of La, Ce, Pr, Sm, Lu, and Dy at F3 between suspended hydrous metal oxide and the aqueous solution.

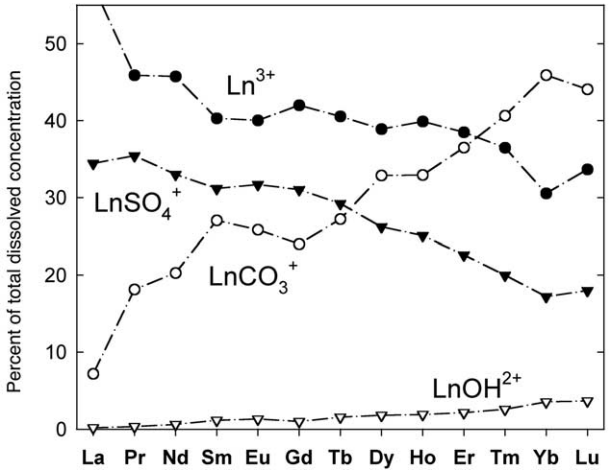


Fig. 9. Aqueous speciation of REE based on the 24-h average composition of Fisher Creek water at F3.

## 5. DISCUSSION

### 5.1. Aqueous Speciation of REE

To help evaluate possible mechanisms for diel cycling and solid-phase partitioning of REE in Fisher Creek, the aqueous speciation of REE in Fisher Creek was investigated using the program Visual Minteq (version 2.2, a recent adaption of the original code written by Allison et al., 1991). The Visual Minteq database contains thermodynamic data for most of the common REE solids (oxides, hydroxides, carbonates, phosphates) as well as the principal aqueous species (complexes with carbonate, sulfate, and hydroxide ligands). The database was amended to include recent thermodynamic data on the 1:1 REE-carbonate (Liu and Byrne, 1998), REE-sulfate (Schijf and Byrne, 2004), and REE-hydroxide (Klungness and Byrne, 2000) complexes.

The 24-h average concentrations of all dissolved constituents at F3 were entered into Visual Minteq, and the aqueous speciation for each REE was computed. The results (Fig. 9) indicate that the predominate aqueous species were $Ln^{3+}$, $LnCO_3^+$, and $LnSO_4^+$, with most of the remaining Ln present as the first hydrolysis species, $LnOH^{2+}$. The percentage of each REE as the uncomplexed $Ln^{3+}$ ion decreased across the lanthanide series, whereas the percentage as the 1:1 carbonate complex increased. However, even for the heavy REE, carbonate complexes never exceeded 46% of the total dissolved REE. The relatively weak degree of REE-carbonate complexation is to be expected given the very low alkalinity of Fisher Creek water. In all cases, essentially all of the dissolved REE were present as cations. Therefore, in terms of adsorption behavior, the REE would be expected to behave in a similar manner as other cationic metals (such as $Cu^{2+}$, $Mn^{2+}$, $Zn^{2+}$).

To test for the effect of diel changes in temperature or major element composition on REE speciation, separate input files were created for the coldest (0800 hours) and warmest (1700 hours) water samples of the 24-h period. Results for selected lanthanide elements (Table 2) illustrate that the changes in predicted aqueous speciation were small, consisting of a slight increase in predominance of the $LnSO_4^+$ and $LnCO_3^+$ ion pairs in warm vs. cold water.

Table 2. Changes in aqueous speciation of selected REE with temperature.

| | | % of dissolved REE | | | |
|---|---|---|---|---|---|
| REE | T, °C | $Ln^{3+}$ | $LnCO_3^+$ | $LnSO_4^+$ | $LnOH^{2+}$ |
| La | 5.0 | 54.0 | 6.0 | 38.7 | 0.8 |
| | 16.7 | 46.6 | 7.0 | 44.9 | 0.8 |
| Sm | 5.0 | 41.8 | 25.0 | 31.7 | 1.2 |
| | 16.7 | 34.1 | 27.6 | 36.1 | 1.8 |
| Dy | 5.0 | 33.5 | 25.2 | 36.7 | 4.6 |
| | 16.7 | 27.1 | 27.5 | 41.4 | 3.8 |
| Lu | 5.0 | 32.7 | 38.1 | 21.7 | 7.0 |
| | 16.7 | 26.8 | 42.2 | 24.4 | 6.0 |

The changes in aqueous speciation of the REE noted above cannot explain the large diel changes in dissolved REE concentration at F3, nor do they help to explain the systematic variation in the partitioning of REE between the solid and aqueous phases (Fig. 7). Previous workers have suggested selective complexation of the heavy REE by carbonate ions to explain the weaker tendency of heavy REE (relative to light REE) to adsorb onto hydrous Fe and Mn precipitates forming in seawater (Koeppenkastrop and DeCarlo, 1992). The opposite pattern is shown in Fisher Creek. However, Verplanck et al. (2004) used theoretical modeling to show that fractionation of REE could occur between acidic water and secondary HFO precipitates, even in the absence of any systematic difference in aqueous speciation across the lanthanide series.

### 5.2. Saturation Indices of REE Solids

It is possible that REE concentrations at F3 were not limited by sorption but rather were controlled by precipitation of a REE phase. Results of Visual Minteq modeling showed that all of the common REE-oxide, -hydroxide, and -carbonate solids were highly undersaturated, by at least five orders of magnitude. Although the modeled saturation indices assumed pure end-member phases, incorporation of a solid-solution model likely would not have changed the conclusion that these solids could not have been present in Fisher Creek.

Based on recent studies of REE transport in surface water, another phase that could impart a solubility control would be a REE-phosphate compound (Sholkovitz 1992, 1995; Byrne and Kim, 1993). However, P was not detected in Fisher Creek water by ICP-MS or ICP-AES methods. Most likely, the concentration of soluble phosphate was fixed at very low levels by adsorption onto the abundant HFO precipitates found in all reaches of Fisher Creek. Nonetheless, to explore the potential importance of REE-phosphate compounds, we assumed an arbitrary value of 1 $\mu$g/L for P, which is $\sim$10 times less than the IDL for the ICP. Using the 24-h average REE concentrations from F3, solubility-product data for the end-member $LnPO_4$ solids from Liu and Byrne (1997), and the assumed P concentration, the Visual Minteq results showed a trend of decreasing saturation index across the lanthanide series (Fig. 10). Even at an assumed low total dissolved P concentration of 1 $\mu$g/L, most of the $LnPO_4$

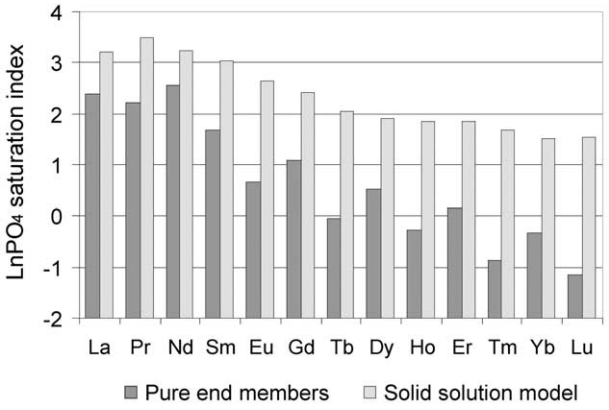


Fig. 10. Trends in the saturation indices of $LnPO_4$ solids at F3. These calculations are based on 24-h average dissolved REE concentrations, and assume an arbitrary concentration of dissolved P = 1 $\mu$g/L. Changing the P concentration changes the value of the indices but does not change the relative trends displayed across the lanthanide series. The solid bars assume pure $LnPO_4$ end-members; the stippled bars assume an ideal solid-solution model. Data for $LnPO_4$ solubility products were taken from Liu and Byrne (1997).

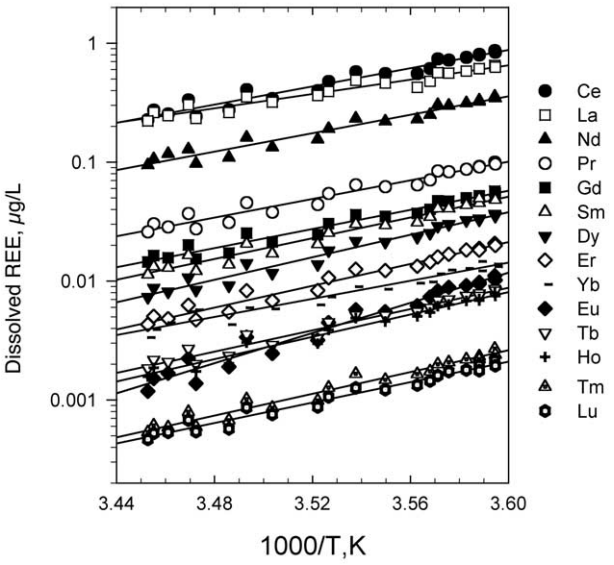


Fig. 11. Relation between dissolved REE concentration and reciprocal temperature (Kelvin) at F3. The slopes of the trend line for each REE can be used to approximate the enthalpy of adsorption onto secondary mineral precipitates. Reciprocal temperature scale is multiplied by 1,000.

solids were predicted to be supersaturated in F3 water, underscoring the very low solubility of these phases. It is important to note that, although the values of the saturation indices shown in Figure 10 are highly sensitive to the chosen total P concentration, the interelement trends are not. It also is possible that dissolved phosphate concentrations followed a diel concentration pattern at F3. Without actual P concentration data, this possibility cannot be evaluated further.

The potential importance of phosphate precipitates was refined by assuming that any hypothetical $LnPO_4$ precipitate would most likely be a solid solution incorporating all of the REE, as is the case for naturally occurring monazite minerals. The 24-h average concentration of each REE in the particulate fraction at F3 was divided by its atomic mass, and the mole fraction of each end-member in the hypothetical $LnPO_4$ solid solution was calculated. Next, the calculated saturation index for each $LnPO_4$ component was adjusted to account for the reduction in activity of the solid end-members. In lieu of a more sophisticated approach, an ideal solid solution model was used such that $\alpha_{LnPO4} = X_{LnPO4}$. Again, the results showed a pattern of decreasing saturation index across the lanthanide series (Fig. 10), although the trend is smoother and less steep as compared to the end-member model.

Whether an end-member or solid-solution model is used, the fact that the heavy REE are predicted to be less saturated with a solid phosphate phase than the light REE is incompatible with the trends in solid-phase partitioning noted in Figure 7. If the light $LnPO_4$ components were more supersaturated than their heavy $LnPO_4$ counterparts, then the suspended solids should have been enriched in the light REE, not the heavy REE (as was observed). These contradictory trends are indirect evidence that weigh against the hypothesis that solid-aqueous partitioning of REE in Fisher Creek is controlled by precipitation of an $LnPO_4$ phase.

### 5.3. Adsorption of REE onto Hydrous Fe and Al Oxides

Previous workers have proposed that pH- and/or temperature-dependent sorption processes play a critical role in diel cycling of arsenic and trace metals in streams (Fuller and Davis, 1989; Nimick et al., 1998; 2003; Gammons et al., 2005). Although the pH dependence of sorption processes is well known (e.g., Dzombak and Morel, 1990), it is less widely recognized that sorption reactions also are sensitive to changes in temperature, despite numerous experimental studies that have quantified this effect (Hodgson et al., 1964; Foda et al., 1982; Johnson, 1990; Machesky, 1990; Barrow, 1992; Rodda et al., 1996; Angove et al., 1998; Trividi and Axe, 2000, 2001; Scheckel and Sparks, 2001). In the case of Fisher Creek, the diel pH change at any one location was very small (only 0.06 log units at F3), whereas the diel temperature change was large (11.7°C at F3). If the diel changes in REE concentration at F3 were indeed sorption related, then it follows that temperature probably played a greater role than pH in generating the observed cycles.

Machesky (1990) derived the following equation that describes the temperature dependence of the residual concentration of a dissolved solute in equilibrium with a solid surface on which it is actively adsorbing:

$$\Delta H_{ads} = 2.303R\left[\log(C_2) - \log(C_1)\right] / \left(1/T_2 - 1/T_1\right) \quad (2)$$

where $\Delta H_{ads}$ is the adsorption enthalpy (J $mol^{-1}$), R is the gas constant (8.3144 J $K^{-1}$ $mol^{-1}$), and $C_1$ and $C_2$ are the dissolved metal concentrations at $T_1$ and $T_2$, where T is in degrees Kelvin. Following equation (2), the slope of a line plotting log(C) vs. 1/T can be used to derive the value of $\Delta H_{ads}$. Figure 11 shows the trends from F3 for each lanthanide element, and Table 3 gives the derived slopes, $r^2$ values, and adsorption

Table 3. Parameters used to estimate $\Delta H_{ads}$ from the data in Figure 11. Units of $\Delta H_{ads}$ are kJ/mol.

| REE | slope | $r^2$ | $\Delta H_{ads}$ |
|---|---|---|---|
| La | 2990 | 0.942 | 57 |
| Ce | 3800 | 0.953 | 73 |
| Pr | 3890 | 0.957 | 74 |
| Nd | 3850 | 0.952 | 74 |
| Sm | 4340 | 0.961 | 83 |
| Eu | 6320 | 0.962 | 120 |
| Gd | 4000 | 0.964 | 77 |
| Tb | 4460 | 0.964 | 85 |
| Dy | 4720 | 0.969 | 90 |
| Ho | 4680 | 0.968 | 90 |
| Er | 4580 | 0.969 | 88 |
| Tm | 4560 | 0.963 | 87 |
| Yb | 3790 | 0.944 | 73 |
| Lu | 4300 | 0.970 | 82 |

enthalpies. In all cases, the correlation between log(C) and reciprocal temperature was excellent ($r^2 > 0.94$). The average value of $\Delta H_{ads}$ for all 14 lanthanides was $+82 \pm 14$ kJ/mol (error denotes one standard deviation). In general, the light REE had smaller enthalpies (especially La, with $\Delta H_{ads} = +57$ kJ/mol), whereas the value for Eu was anomalously large ($\Delta H_{ads} = +120$ kJ/mol). The conditional enthalpy values determined in this study are similar to values reported in the literature for adsorption of divalent metal cations onto hydrous metal oxides. For example, Trividi and Axe (2000) determined enthalpies of +67 to +105 kJ/mol for adsorption of Cd and Zn onto hydrous oxides of Al, Fe, and Mn. Koeppenkastrop (1992) examined the uptake of REE from seawater by FeOOH and $MnO_2$ solids at 2°C, 25°C, and 40°C and reported enthalpies of adsorption for Eu of +24 to +33 kJ/mol. Although these values are considerably lower than those obtained in our study, this could be attributed to differences between the chemistry of seawater and Fisher Creek, especially with respect to pH and carbonate ligand concentration.

It is stressed that the enthalpy values listed in Table 3 should be treated with caution for several reasons. First, the suspended solids onto which the REE are adsorbing in Fisher Creek are a mixture of several different phases; HFO and HAO are probably the most abundant but by no means the only solids present. Second, complete equilibrium was assumed to calculate the enthalpy values. This condition is unlikely to be realized in a stream such as Fisher Creek where pH is rapidly changing with distance downstream and where REE concentrations change rapidly on time scales of minutes to hours. Presumably, adsorption of REE onto hydrous oxide would be faster in warm as opposed to cold water, which would serve to reinforce the trends of lower REE concentration during the afternoon than during the night. Another problem is the implicit assumption that all intensive parameters (other than temperature) that could affect the sorption process were invariant with time. Although pH changes at F3 were very small (total range of 0.06 pH units), the changes did follow a diel cycle in a way that would serve to reinforce the aforementioned temperature effect. In other words, as the temperature of water at F3 increased, the pH also rose slightly. Finally, as shown by Gammons et al. (2005), the mass of HFO produced in the reach upstream from F3 was greater in the afternoon than in the morning and night, meaning that there were more fresh HFO surfaces available for adsorption in the afternoon. Concentrations of HAO also followed a diel cycle. However, as was previously shown (section 4.4 and Fig. 7), the values of $K_d$* (the conditional distribution coefficient between solid and aqueous solution) were strongly temperature dependent, even after the results were normalized to the concentration of suspended HFO particles. The temporal patterns in $K_d$* values are evidence in support of the hypothesis that temperature-dependent sorption processes played a critical role in diel cycling of REE at Fisher Creek.

### 5.4. Comparison with Previous Studies

In a recent investigation of REE in acid mine waters, Verplanck et al. (2004) concluded that the REE behave conservatively where pH is less than 5.1, but begin to partition strongly onto HFO at a pH between 5.1 and 6.6. Furthermore, Verplanck et al. (2004) found that the heavy REE tended to partition into freshly formed HFO to a greater extent than the light REE. Both of these observations are compatible with our results from Fisher Creek. This agreement is not surprising, as the main field site used by Verplanck and coworkers—Uncle Sam Gulch, Montana—shares many similarities with Fisher Creek. Both streams are similar in size, are strongly acidic in their headwaters owing to mine drainage, have abundant HFO formed by $Fe^{2+}$ oxidation, and have downstream increases in pH (Kimball et al., 1999, 2004).

Other workers (e.g., Bau, 1999; Ohta and Kawabe, 2001) have shown experimentally that heavy REE partition more strongly than light REE onto HFO. Ohta and Kawabe (2001) obtained log $K_d$ values of 3 to 4.5 in the pH range 5.6 to 6.6, and illustrated that $K_d$ values for REE were roughly one order of magnitude greater when the lanthanides were coprecipitated with HFO, compared to when they were adsorbed onto previously prepared FeOOH. In a similar study, Koeppenkastrop and De Carlo (1992) reported $K_d$ values of $10^5$ to $10^6$ for partitioning of REE between seawater and amorphous HFO and goethite at pH 7.9. Although the Koeppenskastrop and De Carlo (1992) study showed a trend of decreasing $K_d$ value across the lanthanide series, the opposite trend was noted in similar experiments conducted at lower pH (De Carlo et al., 1998). This difference in sorption behavior may be due to the much greater degree of REE complexation with carbonate ions in seawater. In a recent study of REE geochemistry in a highly acidic (pH 2.6) mining pit lake, Gammons et al. (2003) found that the REE partitioned weakly into freshly formed HFO (formed by oxidation of $Fe^{2+}$) and that the degree of partitioning into the solid phase generally decreased across the lanthanide series. Although the latter trend is again contrary to that observed in Fisher Creek and Uncle Sam Gulch, the Berkeley pit lake studied by Gammons et al. (2003) has a unique chemistry, with extremely high concentrations of sulfate, iron, and other metals (such as Zn, Cu, and Mn) as well as a lower pH than that of Fisher Creek.

Many previous workers have documented the occurrence of middle and (less frequently) heavy REE enrichments in acidic waters when the REE concentrations are normalized to NASC (Bundy et al., 1996; Johannesson et al., 1996; Leybourne et al., 1998; Elbaz-Poulichet and Dupuy, 1999; Johannesson and Zhou, 1999; Verplanck et al., 1999; Gimeno et al., 2000; Worrall and Pearson, 2001a, b; Gammons et al., 2003). However, the Fisher Creek results show a trend of decreasing REE abundance across

the lanthanide series (Fig. 5). In addition, field data summarized in Verplanck et al. (2004) from Uncle Sam Gulch show a general depletion in the middle REE as compared to La and the heavy REE. Thus, it would appear that—whereas middle REE-enrichments are often present in acid waters—such enrichments are by no means a universal phenomenon.

## 6. SUMMARY

The most significant result of this study is the discovery of diel fluctuations in dissolved and particulate REE concentrations in a stream in which hydrous metal oxides were actively precipitating in response to downstream increases in pH. The diel variations in REE concentrations were shown to be quite large (on average, about a fivefold increase in dissolved REE concentration during the night) at the most downstream monitoring station, which had an average 24-h pH of 6.8. Most of the REE lost from solution during the day partitioned into suspended particles such that the total REE concentration showed smaller diel changes (27%–55% increase at night). Conditional distribution coefficients quantifying the partitioning of REE between suspended hydrous Fe and Al oxide particles and aqueous solution were shown to increase during the day and decrease at night. These changes are believed to be due to temperature-dependent adsorption reactions, as the diel variation in pH in Fisher Creek was very small (0.06 log units). Empirically derived adsorption enthalpies for most of the REE ranged from +73 to +90 kJ/mol, and are similar to enthalpies reported in the literature for adsorption of divalent metal cations onto clays and hydrous metal oxides. The light REE partitioned into suspended particles to a lesser degree than the middle and heavy REE, consistent with the recent work of Verplanck et al. (2004). For this reason, shale-normalized profiles of dissolved REE concentrations developed a negative slope across the lanthanide series that steepened during the afternoon hours.

The results of this study clearly show that caution should be used in any attempt to use REE as hydrogeochemical tracers in acid mine waters. Not only can the REE behave in a nonconservative fashion, but REE-attenuating reactions also may occur to different extents depending on the time of day, resulting in strong diel concentration cycles. Indeed, any surface water may show temperature- and/or pH-dependent diel cycling of REE, provided that lanthanide mobility is controlled by adsorption onto clay or hydrous metal oxide. The magnitude of the diel concentration cycle is likely to be greatest in streams where HFO, HAO, or other sorbent phases are actively precipitating and where pH is above the adsorption edge for REE. In such cases, the shape of REE profiles of samples collected in the morning may differ in detail to samples collected in the late afternoon, further complicating use of REE as tracers.

*Acknowledgments*—This study was supported by EPA-EPSCoR, the Montana Board of Research and Commercialization, the U. S. Geological Survey Toxic Substances Hydrology Program, and the USDA Forest Service. The manuscript benefited from technical reviews by Phil Verplanck, Richard Wanty, Karen Johannesson, Jerome Viers, and an anonymous reviewer. Special thanks are due to Bethany Nelson, who performed the REE analyses and assisted with the data reduction. The use of firm, trade, or brand names in this paper is for identification purposes only and does not constitute endorsement by the U. S. Geological Survey.

*Associate editor:* G. Helz.

## REFERENCES

Allison J. D., Brown D. S., and Novo-Gradac K. J. (1991) MINTEQA2/PRODEFA2, a geochemical assessment model for environmental systems: Version 3.0 users manual. Environmental Research Laboratory, U. S. Environmental Protection Agency.

Amacher M. C. (1998) Metal loadings and metals in sediments and wetland soils in the Fisher and Daisy Creek Catchments in the New World Mining District, Montana: A draft assessment report prepared for USDA-FS Region 1 and the US-EPA. Forestry Sciences Lab., USDA-FS-RMRS, Logan, UT.

Amacher M. C., Brown R. W., Kotuby-Amacher J., and Willis A. (1993) Adding sodium hydroxide to study metal removal in a stream affected by acid mine drainage. USDA-FS, Research Paper INT-465.

Amacher M. C., Brown R. W., Sidle R. C. and Kotuby-Amacher J. (1995) Effect of mine waste on element speciation in headwater streams. In *Metal Speciation and Contamination of Soil* (eds. H. E. Allen, C. P. Huang, G. W. Bailey and A. R. Bowers), pp. 275–309. Lewis, Ann Arbor, Mich.

Angove M. J., Johnson B. B., and Wells J. D. (1998) The influence of temperature on the adsorption of cadmium (II) and cobalt (II) on kaolinite. *J. Colloid Interface Sci.* **204,** 93–103.

Åström M. (2001) Abundance and fractionation patterns of rare earth elements in streams affected by acid sulphate soils. *Chem. Geol.* **175,** 249–258.

Baes C. F., and Mesmer R. E. (1981) The thermodynamics of cation hydrolysis. *Am. J. Sci.* **281,** 935–962.

Barrow N. J. (1992) A brief discussion on the effect of temperature on the reaction of inorganic ions with soil. *J. Soil Sci.* **43,** 37–45.

Bau M. (1999) Scavenging of dissolved yttrium and rare earths by precipitating iron oxyhydroxide; experimental evidence for Ce oxidation, Y-Ho fractionation and lanthanide tetrad effect. *Geochim. Cosmochim. Acta* **63,** 67–77.

Brick C. M. and Moore J. N. (1996) Diel variation of trace metals in the upper Clark Fork River, Montana. *Environ. Sci. Technol.* **30,** 1953–1960.

Bundy M. E., Oreskes N., and Hanchar J. M. (1996) Origin of convex-upward REE trends in bog seep and mine effluent waters in Paradise Basin, San Juan Mountains, CO. *Geol. Soc. Amer. Abst. Prog.* **28,** A-469.

Byrne R. H., and Kim K. H. (1993) Rare earth precipitation and coprecipitation behavior: The limiting role of $PO_4^{3-}$ on dissolved rare earth concentrations in seawater. *Geochim. Cosmochim. Acta* **57,** 519–526.

De Carlo E. H., Wen X.-Y., and Irving M. (1998) The influence of redox reactions on the uptake of dissolved Ce by suspended Fe and Mn oxide particles. *Aquat. Geochem.* **3,** 357–389.

Dzombak D. A. and Morel F. A. A. (1990) *Surface Complexation Modeling.* John Wiley, Hoboken, N. J.

Elbaz-Poulichet F., and Dupuy C. (1999) Behavior of rare earth elements at the freshwater-seawater interface of two acid mine rivers: the Tinto and Odiel (Andalusia, Spain). *Applied Geochem.* **14,** 1063–1072.

Elliot J. E., Kirk A. R., and Johnson T. W. (1992) Field guide; gold-copper-silver deposits of the New World district. *Northwest Geol.* **20–21**, 1–20.

Foda M. S., El-Kadi H. A., El-Demerdashe S., and Abdel-Hamid E. A. (1982) Effect of temperature on manganese adsorption by clay minerals. *Egypt. J. Soil Sci.* **22,** 23–29.

Fuller C. C. and Davis J. A. (1989) Influence of coupling of sorption and photosynthetic processes on trace elements cycles in natural waters. *Nature* **340,** 52–54.

Gammons C. H., Wood S. A., Jonas J. P., and Madison J. P. (2003) Geochemistry of rare earth elements and uranium in the acidic Berkeley Pit lake, Butte, Montana. *Chem. Geol.* **198,** 269–288.

Gammons C. H., Nimick D. A., Parker S. R., Cleasby T. E., and McCleskey R. B. (2005) Diel behavior of Fe and other heavy metals in a mountain stream with acidic to neutral pH: Fisher Creek, Montana, USA. *Geochim. Cosmochim. Acta.*

Gimeno M. J., Auqué L. F., and Nordstrom D. K. (2000) REE speciation in low-temperature acidic waters and the competitive effects of aluminum. *Chem. Geol.* **165,** 167–180.

Gromet L. P., Dymek R. F., Haskin L. A., and Korotev R. L. (1984) The "North American shale composite"; its compilation, major and trace element characteristics. *Geochim. Cosmochim. Acta* **48,** 2469–2482.

Hodgson J. F., Geering H. R., and Fellows M. (1964) The influence of fluoride, temperature, calcium and alcohol on the reaction of cobalt with montmorillonite. *Soil Sci. Soc. Am. Proc.* **28,** 39–42.

Hollings P., Hendry M. J., and Kerrich R. (1999) Sequential filtration of surface and ground waters from the Rabbit Lake uranium mine, northern Saskatchewan, Canada. *Water Qual. Res. J. Can.* **34,** 221–247.

Johnson B. B. (1990) Effect of temperature and concentration on the adsorption of cadmium on goethite. *Environ. Sci. Tech.* **24,** 112–118.

Johannesson K. H. and Lyons W. B. (1995) Rare-earth element geochemistry of Colour Lake, an acidic freshwater lake on Axel Heiberg Island, Northwest Territories, Canada. *Chem. Geol.* **119,** 209–223.

Johannesson K. H. and Xiaoping Z. (1999) Origin of middle rare earth element enrichments in acid waters of a Canadian High Arctic lake. *Geochim. Cosmochim. Acta* **63,** 153–165.

Johannesson K. H., Lyons W. B., Yelken M. A., Gaudette H. E., and Stetzenbach K. J. (1996) Geochemistry of rare earth elements in hypersaline and dilute acidic natural terrestial waters: Complexation behavior and middle rare-earth element enrichments. *Chem. Geol.* **133,** 125–144.

Jones C. A., Nimick D. A., and McCleskey R. B. (2004) Relative effect of temperature and pH on diel cycling of dissolved trace elements in Prickly Pear Creek, Montana. *Water Air Soil Poll.* **153,** 95–113.

Kimball B. A., Nimick D. A., Gerner L. J., and Runkel R. L. (1999) Quantification of metal loading in Fisher Creek by tracer injection and synoptic sampling, Park County, Montana, August 1997. *U. S. Geol. Surv Wat. Resour. Invest. Rep.* 99–4119.

Kimball , B. A., Runkel , R. L., Cleasby , T. E. and Nimick, D. A. (2004) Quantification of metal loading by tracer injection and synoptic sampling, 1997–1998. In *Integrated investigation of environmental effects of historical mining in the Basin and Boulder mining districts, Boulder River watershed, Jefferson County, Montana* (eds. D. A. Nimick, S. E. Church and S. E. Finger), chap. D6. U. S. Geological Survey Professional Paper 1652.

Klungness G. D. and Byrne R. H. (2000) Comparative hydrolysis of the rare earth elements and yttrium: The influence of temperature and ionic strength. *Polyhedron* **19,** 99–107.

Koeppenkastrop D. (1992) *Thermodynamic and kinetic studies on the interaction of rare earth elements with metal oxides.* Ph.D. Dissertation, Univ. Hawaii, 409 pp.

Koeppenkastrop D. and De Carlo E. H. (1992) Sorption of rare-earth elements from seawater onto synthetic mineral particles: An experimental approach. *Chem. Geol.* **95,** 251–263.

Lewis A. J., Palmer M. R., Sturchio N. C., and Kemp A. J. (1997) The rare earth element geochemistry of acid-sulphate and acid-sulphate-chloride geothermal systems from Yellowstone National Park, Wyoming, USA. *Geochim. Cosmochim. Acta* **61,** 695–706.

Leybourne M. I., Goodfellow W. D., and Boyle D. R. (1998) Hydrogeochemical, isotopic and rare earth element evidence for contrasting water-rock interactions at two undisturbed Zn-Pb massive sulphide deposits, Bathurst Mining Camp, N.B., Canada. *J. Geochem. Explor.* **64,** 237–261.

Leybourne M. I., Goodfellow W. D., Boyle D. R., and Hall G. M. (2000) Rapid development of negative Ce anomalies in surface waters and contrasting REE patterns in groundwaters associated with Zn-Pb massive sulphide deposits. *Appl. Geochem.* **15,** 695–723.

Liu X. and Byrne R. H. (1997) Rare earth and yttrium phosphate solubilities in aqueous solution. *Geochim. Cosmochim. Acta* **61,** 1625–1633.

Liu X. and Byrne R. H. (1998) Comprehensive investigation of yttrium and rare earth element complexation by carbonate ions using ICP-MS spectrometry. *J. Soln. Chem.* **27,** 803–815.

Machesky M. L. (1990) Influence of temperature on ion adsorption by hydrous metal oxides. In *Chemical modeling of aqueous systems I* (eds. R. L. Bassett and D. C. Melchoir), pp. 282–292. American Chemical Symposium Series 416.

McKnight D. M. and Bencala K. E. (1989) Reactive iron transport in an acidic mountain stream in Summit County, Colorado: A hydrologic perspective. *Geochim. Cosmochim. Acta* **53,** 2225–2234.

McKnight D. M., Kimball B. A., and Bencala K. E. (1988) Iron photoreduction and oxidation in an acidic mountain stream. *Science* **240,** 637–640.

McKnight D. M., Kimball B. A., and Runkel R. L. (2001) pH dependence of iron photoreduction in a rocky mountain stream affected by acid mine drainage. *Hydrol. Proc.* **15,** 1979–1992.

Miekeley N., Couthino de Jesus H., Porto da Silveira C. L., Linsalata P., and Morse R. (1992) Rare-earth elements in groundwaters from the Osamu Utsumi mine and Morro do Ferro analogue study sites, Poços de Caldas, Brazil. *J. Geochem. Explor.* **45,** 365–387.

Nimick D. A., Moore J. N., Dalby C. E., and Savka M. W. (1998) The fate of geothermal arsenic in the Madison and Missouri Rivers, Montana and Wyoming. *Wat. Resour. Res.* **34,** 3051–3067.

Nimick D. A., Gammons C. H., Cleasby T. E., Madison J. P., Skaar D., and Brick C. M. (2003) Diel cycles in dissolved metal concentrations in streams—occurrence and possible causes. *Wat. Resour. Res.* **39,** 1247. doi:10.1029/WR001571

Nimick D. A., Cleasby T. E., and McLeskey, R. B. (2005) Seasonality of diel cycles of dissolved trace-metal concentrations in a Rocky Mountain stream: *Environ. Geol.* **47,** 603–614.

Ohta A. and Kawabe I. (2001) REE(III) adsorption onto Mn dioxide ($\delta$-$MnO_2$) and Fe oxyhydroxide: Ce(III) oxidation by $\delta$-$MnO_2$. *Geochim. Cosmochim. Acta* **65,** 695–704.

Rodda D. P., Johnson B. B., and Wells J. D. (1996) Modeling the effect of temperature on adsorption of lead(II) and zinc(II) onto goethite at constant pH. *J. Colloid Interface Sci.* **184,** 365–377.

Scheckel K. G. and Sparks D. L. (2001) Temperature effects on nickel sorption kinetics at the mineral-water interface. *Soil Sci. Soc. Am. J.* **65,** 719–728.

Schijf J. and Byrne R. H. (2004) Determination of $_{SO4}\beta_1$ for yttrium and the rare earth elements at $I = 0.66m$ and t = 25°C—implications for YREE solution speciation in sulfate-rich waters. *Geochim. Cosmochim Acta* **68,** 2825–2837.

Sholkovitz E. R. (1992) Chemical evolution of rare earth elements: fractionation between colloidal and solution phases of filtered river water. *Earth Planet. Sci. Letters* **114,** 77–84.

Sholkovitz E. R. (1995) The aquatic chemistry of rare earth elements in rivers and estuaries. *Aquatic Geochem.* **1,** 1–34.

Sullivan A. B., Drever J. I., and McKnight D. M. (1998) Diel variation in element concentrations, Peru Creek, Summit County, Colorado. *J. Geochem. Explor.* **64,** 141–145.

Sverjensky D. A. (1984) Europium redox equilibria in aqueous solution. *Earth Planet. Sci. Lett.* **67,** 70–78.

Trividi P. and Axe L. (2000) Modeling Cd and Zn sorption to hydrous metal oxides. *Environ. Sci. Tech.* **34,** 2215–2223.

Trividi P. and Axe L. (2001) Predicting divalent metal sorption to hydrous Al, Fe and Mn oxides. *Environ. Sci. Tech.* **35,** 1779–1784.

Verplanck P. L., Nordstrom D. K., and Taylor H. E. (1999) Overview of rare earth element investigations in acid waters of U. S. Geological Survey abandoned mine lands watersheds. *U. S. Geol. Surv. Wat. Resour. Invest. Rep.* 99–4018A, pp. 83–92.

Verplanck P. L., Nordstrom D. K., Taylor H. E., and Kimball B. A. (2004) Rare earth element partitioning between hydrous ferric oxides and acid mine water during iron oxidation. *Applied Geochem.* **19,** 1339–1354.

Wood S. A., Shannon W. M., and Baker L. L. (in press) The aqueous geochemistry of the rare earth elements and yttrium. Part 13: REE geochemistry of mine drainage from the Pine Creek area, Coeur d'Alene River valley, Idaho, USA. In *Rare Earth Elements in Groundwater Flow Systems* (ed. K. H. Johannesson). Water Science and Technology Library v.51, Springer, Dordrecht, The Netherlands, p. 89–110.

Worrall F. and Pearson D. G. (2001a) The development of acidic groundwater in coal-bearing strata: Part 1. Rare earth element fingerprinting. *Applied Geochem.* **16,** 1465–1480.

Worrall F. and Pearson D. G. (2001b) Water-rock interaction in an acidic mine discharge as indicated by rare earth element patterns. *Geochim. Cosmochim. Acta* **65,** 3027–3040.

## APPENDIX

Table A1. REE analyses of samples collected at Fisher Creek on 8/13 and 8/14/2002. All concentration data are in μg/L. FA = Filtered (0.1 μm)-acidified; RA = raw-acidified; uFA = ultrafiltered (0.001 μm)-acidified. Values in italics were less than the instrument detection limit, and therefore are of lower reliability. This was mainly a problem for FA samples for Lu from F3.

| Sample | Date and time | T, °C | pH | La/139 | Ce/140 | Pr/141 | Nd/146 | Sm/147 | Eu/151 | Gd/157 | Tb/159 | Dy/163 | Ho/165 | Er/166 | Tm/169 | Yb/174 | Lu/175 |
|---|---|---|---|---|---|---|---|---|---|---|---|---|---|---|---|---|---|
| Instrument detection limit | | | | 0.0007 | 0.0012 | 0.0005 | 0.0004 | 0.0003 | 0.0019 | 0.001 | 0.0003 | 0.0004 | 0.0002 | 0.0003 | 0.0004 | 0.0005 | 0.0019 |
| *F1 Site:* | | | | | | | | | | | | | | | | | |
| F1-1 FA | 8/13 11:00 | 7.5 | 6.83 | 4.68 | 9.77 | 1.18 | 4.73 | 0.857 | 0.215 | 1.00 | 0.148 | 0.840 | 0.162 | 0.457 | 0.0560 | 0.337 | 0.0452 |
| F1-1 RA | | | | 4.79 | 10.0 | 1.20 | 4.80 | 0.867 | 0.218 | 1.02 | 0.151 | 0.857 | 0.165 | 0.466 | 0.0571 | 0.349 | 0.0462 |
| F1-9 FA | 8/13 19:00 | 14.8 | 6.83 | 4.69 | 9.71 | 1.15 | 4.52 | 0.814 | 0.201 | 1.01 | 0.150 | 0.857 | 0.164 | 0.458 | 0.0563 | 0.336 | 0.0452 |
| F1-9 RA | | | | 4.81 | 9.93 | 1.17 | 4.63 | 0.831 | 0.206 | 1.09 | 0.159 | 0.893 | 0.171 | 0.482 | 0.0584 | 0.348 | 0.0466 |
| F1-17 FA | 8/14 3:00 | 6.5 | 6.78 | 4.84 | 9.95 | 1.19 | 4.75 | 0.860 | 0.215 | 1.01 | 0.148 | 0.864 | 0.166 | 0.440 | 0.0579 | 0.346 | 0.0461 |
| F1-17 RA | | | | 4.97 | 10.3 | 1.24 | 4.94 | 0.893 | 0.226 | 1.03 | 0.151 | 0.884 | 0.171 | 0.453 | 0.0598 | 0.356 | 0.0475 |
| *F2 Site:* | | | | | | | | | | | | | | | | | |
| F2-1 FA | 8/13 11:00 | 7.5 | 6.83 | 1.43 | 2.62 | 0.328 | 1.25 | 0.221 | 0.0544 | 0.253 | 0.0372 | 0.215 | 0.0420 | 0.111 | 0.0146 | 0.0828 | 0.0117 |
| F2-1 RA | | | | 1.46 | 2.71 | 0.342 | 1.33 | 0.240 | 0.0582 | 0.272 | 0.0389 | 0.230 | 0.0443 | 0.119 | 0.0154 | 0.0894 | 0.0122 |
| F2-9 FA | 8/13 19:00 | 14.8 | 6.83 | 1.53 | 2.84 | 0.361 | 1.41 | 0.252 | 0.0605 | 0.278 | 0.0394 | 0.231 | 0.0445 | 0.119 | 0.0153 | 0.0902 | 0.0122 |
| F2-9 RA | | | | 1.55 | 2.93 | 0.372 | 1.46 | 0.264 | 0.0647 | 0.294 | 0.0421 | 0.247 | 0.0474 | 0.126 | 0.0164 | 0.0988 | 0.0130 |
| F2-17 FA | 8/14 3:00 | 6.5 | 6.78 | 1.54 | 2.86 | 0.362 | 1.40 | 0.250 | 0.0614 | 0.278 | 0.0396 | 0.236 | 0.0452 | 0.122 | 0.0159 | 0.0927 | 0.0124 |
| F2-17 RA | | | | 1.56 | 2.92 | 0.370 | 1.46 | 0.265 | 0.0648 | 0.295 | 0.0422 | 0.252 | 0.0485 | 0.130 | 0.0168 | 0.101 | 0.0134 |
| *F3 Site:* | | | | | | | | | | | | | | | | | |
| F3-1 FA | 8/13 11:00 | 7.5 | 6.83 | 0.425 | 0.553 | 0.064 | 0.228 | 0.0311 | 0.0062 | 0.037 | 0.0055 | 0.0234 | 0.0050 | 0.0133 | 0.0016 | 0.0096 | *0.0013* |
| F3-1 RA | | | | 0.675 | 1.16 | 0.153 | 0.586 | 0.107 | 0.0240 | 0.123 | 0.0191 | 0.1030 | 0.0197 | 0.0531 | 0.0069 | 0.0412 | 0.0057 |
| F3-2 FA | 8/13 12:00 | 10.4 | 6.82 | 0.391 | 0.476 | 0.054 | 0.190 | 0.0254 | 0.0045 | 0.030 | 0.0045 | 0.0181 | 0.0039 | 0.0106 | 0.0013 | 0.0073 | *0.0011* |
| F3-3 FA | 8/13 13:00 | 13.1 | 6.82 | 0.353 | 0.407 | 0.046 | 0.160 | 0.0206 | 0.0034 | 0.025 | 0.0035 | 0.0141 | 0.0030 | 0.0083 | 0.0010 | 0.0059 | *0.0009* |
| F3-3 RA | | | | 0.620 | 1.10 | 0.147 | 0.564 | 0.103 | 0.0225 | 0.117 | 0.0185 | 0.0964 | 0.0187 | 0.0503 | 0.0068 | 0.0381 | 0.0052 |
| F3-4 uFA | 8/13 14:00 | 15.1 | 6.82 | 0.207 | 0.206 | 0.023 | 0.096 | 0.0103 | 0.0009 | 0.013 | 0.0018 | 0.0066 | 0.0014 | 0.0037 | 0.0006 | 0.0029 | *0.0004* |
| F3-4 FA | | | | 0.304 | 0.333 | 0.037 | 0.128 | 0.0165 | 0.0022 | 0.020 | 0.0027 | 0.0107 | 0.0023 | 0.0062 | 0.0008 | 0.0055 | *0.0007* |
| F3-5 FA | 8/13 15:00 | 16.3 | 6.82 | 0.261 | 0.273 | 0.030 | 0.106 | 0.0132 | 0.0015 | 0.016 | 0.0022 | 0.0088 | 0.0019 | 0.0050 | 0.0006 | 0.0039 | *0.0005* |
| F3-5 RA | | | | 0.604 | 1.10 | 0.149 | 0.568 | 0.103 | 0.0222 | 0.116 | 0.0181 | 0.0961 | 0.0185 | 0.0491 | 0.0066 | 0.0372 | 0.0052 |
| F3-7 FA | 8/13 17:00 | 16.5 | 6.83 | 0.222 | 0.227 | 0.026 | 0.094 | 0.0113 | 0.0012 | 0.014 | 0.0018 | 0.0073 | 0.0016 | 0.0043 | 0.0005 | 0.0033 | *0.0005* |
| F3-7 RA | | | | 0.584 | 1.07 | 0.145 | 0.559 | 0.102 | 0.0219 | 0.113 | 0.0176 | 0.0922 | 0.0186 | 0.0473 | 0.0063 | 0.0361 | 0.0050 |
| F3-8 FA | 8/13 18:00 | 15.8 | 6.83 | 0.246 | 0.254 | 0.028 | 0.117 | 0.0129 | 0.0017 | 0.016 | 0.0021 | 0.0081 | 0.0017 | 0.0048 | 0.0006 | 0.0045 | *0.0005* |
| F3-9 FA | 8/13 19:00 | 14.8 | 6.83 | 0.233 | 0.242 | 0.027 | 0.097 | 0.0121 | 0.0014 | 0.015 | 0.0020 | 0.0084 | 0.0017 | 0.0047 | 0.0006 | 0.0057 | *0.0005* |
| F3-9 RA | | | | 0.526 | 0.949 | 0.129 | 0.495 | 0.0909 | 0.0195 | 0.100 | 0.0155 | 0.0829 | 0.0159 | 0.0422 | 0.0055 | 0.0324 | 0.0044 |
| F3-10 FA | 8/13 20:00 | 13.7 | 6.81 | 0.261 | 0.275 | 0.031 | 0.109 | 0.0138 | 0.0019 | 0.017 | 0.0023 | 0.0092 | 0.0020 | 0.0055 | 0.0007 | 0.0043 | *0.0006* |
| F3-11uFA | 8/13 21:00 | 12.3 | 6.80 | 0.289 | 0.298 | 0.033 | 0.113 | 0.0148 | 0.0018 | 0.018 | 0.0026 | 0.0102 | 0.0023 | 0.0059 | 0.0009 | 0.0047 | *0.0007* |
| F3-11 FA | | | | 0.319 | 0.342 | 0.038 | 0.133 | 0.0170 | 0.0025 | 0.021 | 0.0029 | 0.0117 | 0.0026 | 0.0068 | 0.0009 | 0.0058 | *0.0008* |
| F3-11 RA | | | | 0.590 | 0.997 | 0.134 | 0.512 | 0.0915 | 0.0195 | 0.103 | 0.0162 | 0.0846 | 0.0164 | 0.0440 | 0.0058 | 0.0333 | 0.0045 |
| F3-12 FA | 8/13 22:00 | 10.8 | 6.80 | 0.363 | 0.398 | 0.044 | 0.155 | 0.0204 | 0.0032 | 0.024 | 0.0033 | 0.0138 | 0.0030 | 0.0083 | 0.0010 | 0.0063 | *0.0009* |
| F3-13 FA | 8/13 23:00 | 9.5 | 6.79 | 0.487 | 0.574 | 0.064 | 0.232 | 0.0302 | 0.0057 | 0.036 | 0.0051 | 0.0217 | 0.0049 | 0.0125 | 0.0017 | 0.0089 | *0.0013* |
| F3-13 RA | | | | 0.637 | 1.05 | 0.139 | 0.538 | 0.0981 | 0.0210 | 0.110 | 0.0170 | 0.0905 | 0.0177 | 0.0470 | 0.0062 | 0.0376 | 0.0050 |
| F3-14 FA | 8/14 0:00 | 8.6 | 6.80 | 0.463 | 0.554 | 0.062 | 0.220 | 0.0295 | 0.0055 | 0.035 | 0.0051 | 0.0213 | 0.0046 | 0.0122 | 0.0015 | 0.0085 | *0.0012* |
| F3-16 FA | 8/14 2:00 | 7.1 | 6.78 | 0.478 | 0.611 | 0.071 | 0.249 | 0.0346 | 0.0073 | 0.040 | 0.0059 | 0.0253 | 0.0054 | 0.0144 | 0.0017 | 0.0098 | *0.0014* |
| F3-17 FA | 8/14 3:00 | 6.5 | 6.78 | 0.560 | 0.719 | 0.083 | 0.298 | 0.0407 | 0.0088 | 0.047 | 0.0070 | 0.0301 | 0.0063 | 0.0168 | 0.0021 | 0.0124 | *0.0017* |
| F3-17 RA | | | | 0.798 | 1.26 | 0.162 | 0.616 | 0.111 | 0.0247 | 0.127 | 0.0198 | 0.106 | 0.0207 | 0.0556 | 0.0074 | 0.0436 | 0.0060 |

Table A1. (Continued)

| Sample | Date and time | T, °C | pH | La/139 | Ce/140 | Pr/141 | Nd/146 | Sm/147 | Eu/151 | Gd/157 | Tb/159 | Dy/163 | Ho/165 | Er/166 | Tm/169 | Yb/174 | Lu/175 |
|---|---|---|---|---|---|---|---|---|---|---|---|---|---|---|---|---|---|
| F3-18uFA | 8/14 4:00 | 6.0 | 6.77 | 0.568 | 0.703 | 0.078 | 0.275 | 0.0373 | 0.0079 | 0.044 | 0.0065 | 0.0276 | 0.0058 | 0.0153 | 0.0040 | 0.0103 | *0.0014* |
| F3-18 FA | | | | 0.583 | 0.758 | 0.087 | 0.312 | 0.0436 | 0.0091 | 0.050 | 0.0075 | 0.0324 | 0.0068 | 0.0182 | 0.0022 | 0.0127 | *0.0018* |
| F3-19 FA | 8/14 5:00 | 5.5 | 6.77 | 0.609 | 0.803 | 0.092 | 0.330 | 0.0454 | 0.0097 | 0.052 | 0.0079 | 0.0336 | 0.0070 | 0.0188 | 0.0023 | 0.0146 | 0.0020 |
| F3-19 RA | | | | 0.799 | 1.27 | 0.163 | 0.615 | 0.111 | 0.0248 | 0.128 | 0.0202 | 0.107 | 0.0213 | 0.0558 | 0.0078 | 0.0503 | 0.0065 |
| F3-21 FA | 8/14 7:00 | 5.1 | 6.79 | 0.648 | 0.864 | 0.100 | 0.356 | 0.0497 | 0.0111 | 0.057 | 0.0086 | 0.0367 | 0.0079 | 0.0207 | 0.0027 | 0.0139 | 0.0021 |
| F3-21 RA | | | | 0.810 | 1.31 | 0.168 | 0.642 | 0.116 | 0.0256 | 0.131 | 0.0205 | 0.110 | 0.0217 | 0.0574 | 0.0075 | 0.0443 | 0.0060 |
| F3-22 FA | 8/14 8:00 | 5.0 | 6.80 | 0.629 | 0.838 | 0.096 | 0.344 | 0.0483 | 0.0102 | 0.055 | 0.0083 | 0.0352 | 0.0075 | 0.0198 | 0.0024 | 0.0132 | 0.0019 |
| F3-23 FA | 8/14 9:00 | 5.5 | 6.81 | 0.611 | 0.796 | 0.091 | 0.322 | 0.0496 | 0.0094 | 0.051 | 0.0075 | 0.0328 | 0.0068 | 0.0182 | 0.0022 | 0.0122 | *0.0018* |
| F3-23 RA | | | | 0.781 | 1.27 | 0.162 | 0.622 | 0.111 | 0.0249 | 0.127 | 0.0197 | 0.106 | 0.0209 | 0.0553 | 0.0074 | 0.0425 | 0.0059 |
| F3-24 FA | 8/14 10:00 | 6.9 | 6.82 | 0.565 | 0.738 | 0.084 | 0.302 | 0.0409 | 0.0083 | 0.047 | 0.0069 | 0.0290 | 0.0062 | 0.0159 | 0.0020 | 0.0115 | *0.0016* |
| F3-25 FA | field blank | | | 0.0067 | 0.0084 | 0.0035 | 0.0058 | 0.0009 | *0.0007* | 0.003 | 0.0004 | 0.0010 | 0.0003 | 0.0006 | *0.0003* | 0.0008 | *0.0004* |
| F3-25 RA | field blank | | | 0.0013 | 0.0017 | *0.0004* | 0.0015 | 0.0004 | *0.0011* | 0.001 | *0.0002* | *0.0003* | *0.0001* | *0.0002* | *0.0001* | *0.0004* | *0.0001* |
| F3-26 FA | dup of F3-21 | | | 0.661 | 0.878 | 0.102 | 0.359 | 0.0495 | 0.0087 | 0.067 | 0.0093 | 0.0453 | 0.0096 | 0.0252 | 0.0044 | 0.0168 | 0.0028 |